Atmospheric Chemistry of Pivalaldehyde and Isobutyraldehyde: Kinetics and Mechanisms of Reactions with Cl Atoms, Fate of $(CH_3)_3CC(O)$ and $(CH_3)_2CHC(O)$ Radicals, and Self-Reaction Kinetics of $(CH_3)_3CC(O)O_2$ and $(CH_3)_2CHC(O)O_2$ Radicals

Jean-Paul Le Crâne and Eric Villenave*

Laboratoire de Physico-Chimie Moléculaire, CNRS UMR 5803, Université Bordeaux I, 33405 Talence Cedex, France

Michael D. Hurley and Timothy J. Wallington*

Ford Research Laboratory, MD 3083/SRL, Ford Motor Company, Dearborn, Michigan 48121-2053

Satoshi Nishida, Kenshi Takahashi, and Yutaka Matsumi

Solar-Terrestrial Environment Laboratory and Graduate School of Science, Nagoya University, Japan

Received: September 10, 2003; In Final Form: November 26, 2003

The kinetics and mechanism of the reactions Cl + $(CH_3)_3CCHO$ and Cl + $(CH_3)_2CHCHO$ were investigated at room temperature using two complementary techniques: flash photolysis/UV absorption and continuous photolysis/Fourier transform infrared (FTIR) smog chamber. Reactions proceed predominantly by abstraction of the aldehydic H atom to form acyl radicals. FTIR measurements indicated that the acyl-forming channel accounts for 81% ± 8% and 85% ± 10% of the reaction of Cl atoms with $(CH_3)_3CCHO$ and $(CH_3)_2CHCHO$. UV measurements indicated that the acyl-forming channel accounts for 88% ± 6% and 85% ± 5% of the reaction of Cl atoms with $(CH_3)_3CCHO$ and $(CH_3)_2CHCHO$. The atmospheric fate (>98%) of the resulting $(CH_3)_3CC(O)$ and $(CH_3)_2CHC(O)$ radicals is an addition of O_2 to give the corresponding acylperoxy radical. In 700 Torr of N_2/O_2 mixtures at a temperature of 296 K, the decomposition of $(CH_3)_3CC(O)$ and $(CH_3)_2CHC(O)$ radicals via CO elimination occurs at rates of $\sim 1 \times 10^5$ and $\sim 4 \times 10^3$ s^{-1}, respectively. Relative rate methods were used to measure the reaction rates (in units of cm^3 $molecule^{-1}$ s^{-1}): $k(Cl + (CH_3)_3CCHO) = (1.15 \pm 0.30) \times 10^{-10}$; $k(Cl + (CH_3)_2CHCHO) = (1.33 \pm 0.25) \times 10^{-10}$; $k(Cl + (CH_3)_3CC(O)Cl) = (6.86 \pm 1.50) \times 10^{-12}$; $k(Cl + (CH_3)_2CHC(O)Cl) = (7.82 \pm 2.10) \times 10^{-12}$; $k(Cl + (CH_3)_3CCl) = (1.27 \pm 0.21) \times 10^{-11}$; and $k(Cl + (CH_3)_2CHCCl) = (2.01 \pm 0.49) \times 10^{-11}$. Self-reaction rate constants were measured for $(CH_3)_3CC(O)O_2$ and $(CH_3)_2CHC(O)O_2$ radicals and compared to previous measurements.

1. Introduction

Aldehydes (RCHO) are important trace constituents of the atmosphere. They have natural and anthropogenic sources, with small primary sources that are associated with vehicle exhaust and industrial activity and large secondary sources that are associated with the oxidation of volatile organic compounds.[1,2] Abstraction of the aldehydic H atom by OH radicals gives acyl radicals, RC(O), which combine with O_2 to give acylperoxy radicals, $RC(O)O_2$. Acylperoxy radicals have several important roles in atmospheric chemistry. $RC(O)O_2$ radicals react rapidly with NO to give NO_2, which is then photolyzed, leading to ozone formation. $RC(O)O_2$ radicals react with NO_2 to form stable peroxyacylnitrates, $RC(O)O_2NO_2$. Peroxyacylnitrates are severe irritant compounds in photochemical smog, efficient reservoirs of NO_x in the troposphere, and transport NO_x far from its sources.[3] In air masses with low [NO_x], acylperoxy radicals undergo reactions with HO_2 and other peroxy radicals. Reactions of $RC(O)O_2$ with HO_2 radicals are important radical chain termination reactions and are a source of ozone and carboxylic acids in the atmosphere.

The kinetic database that concerns atmospherically relevant reactions of acylperoxy radicals is limited. Acetaldehyde is often used as the model for the reactivity of aldehydes in chemical modeling of atmospheric chemistry. Prior to a study of the effect of the substitution of H atoms in $CH_3C(O)O_2$ by methyl groups on the reactivity of acylperoxy radicals with HO_2, it is first necessary to characterize a suitable laboratory source of acylperoxy radicals. In laboratory studies, Cl atoms or OH radicals are often used to generate peroxy radicals. Traditional OH radical sources, such as H_2O_2 or HNO_3 photolysis (wavelengths of $\lambda < 300$ nm), are problematic, because the photolysis of aldehydes at $\lambda < 300$ nm[4,5] can complicate the kinetic analysis. Cl atoms are produced readily by photolysis of Cl_2 at $\lambda = 330-360$ nm, where aldehyde photolysis is not a significant problem. The kinetics of the reactions of Cl atoms with aldehydes have been the subject of numerous studies, and the overall reaction kinetics are now reasonably well-established.[6] Unfortunately, with the exception of acetaldehyde, there is little mechanistic information concerning the reaction of the Cl atom with aldehydes. For acetaldehyde, it has been shown that the reaction occurs predominantly (>95%) via abstraction of the aldehydic hydrogen.[7,8]

* Authors to whom correspondence should be addressed. E-mail: e.villenave@lpcm.u-bordeaux1.fr, twalling@ford.com.

10.1021/jp036705f CCC: $27.50
Published on Web 01/10/2004

The objective of the present work was to determine the kinetics and mechanisms of the reactions of Cl atoms with $(CH_3)_3CCHO$ (pivalaldehyde or 2,2-dimethylpropanal) and $(CH_3)_2CHCHO$ (isobutyraldehyde or 2-methylpropanal) and to evaluate their utility as a source of methyl-substituted acyl— and, hence, acyl peroxy—radicals.

$$Cl + (CH_3)_3CCHO \rightarrow HCl + (CH_3)_3CC(O) \quad (1a)$$

$$\rightarrow HCl + (CH_3)_2(CH_2)CCHO \quad (1b)$$

$$Cl + (CH_3)_2CHCHO \rightarrow HCl + (CH_3)_2CHC(O) \quad (2a)$$

$$\rightarrow HCl + CH_3(CH_2)CHCHO \quad (2b)$$

$$\rightarrow HCl + (CH_3)_2CCHO \quad (2c)$$

Branching ratios for reactions 1 and 2 were investigated at room temperature, using two complementary techniques: flash photolysis/UV absorption in Bordeaux, France, and continuous photolysis/Fourier transform infrared (FTIR) smog chamber in Dearborn, Michigan. To assess the possible importance of secondary reactions in the present system, relative rate studies were performed to determine rate constants for the reactions of Cl atoms with $(CH_3)_3CC(O)Cl$, $(CH_3)_2CHC(O)Cl$, $(CH_3)_3CCl$, and $(CH_3)_2CHCCl$. The atmospheric fate of $(CH_3)_3CC(O)$ and $(CH_3)_2CHC(O)$ radicals was determined. Finally, the kinetics of the self-reactions of $(CH_3)_3CC(O)O_2$ and $(CH_3)_2CHC(O)O_2$ radicals were investigated and compared with previous work from our laboratory.[9]

2. Experimental Section

The experimental systems used have been described in detail elsewhere[10,11] and are discussed briefly here.

2.1. Flash Photolysis Experiments. A conventional flash photolysis UV absorption spectrometer was used to monitor peroxy radical absorptions at room temperature and atmospheric pressure. The reaction cell consists of a 70-cm-long, 4-cm-diameter Pyrex cylinder. A continuous flow of reactant gas mixture was irradiated periodically by two argon flash lamps. The analyzing beam was obtained from a deuterium lamp, passed through the cell, dispersed using a monochromator (2-nm resolution), detected by a photomultiplier, and transferred to a personal computer (PC) for averaging and analysis. Scattered light from the flash prevented data from being recorded for ~50−100 μs after the flash. Approximately 30−40 absorption time profiles were acquired to reach a satisfactory signal-to-noise ratio. The total gas flow was adjusted so that the cell was replenished completely between flashes, thereby avoiding photolysis of the reaction products. Decay traces were simulated by numerical integration of a set of differential equations that were representative of an appropriate chemical mechanism, and selected parameters (rate constant, absorption cross section, and initial radical concentration) were adjusted to give the best nonlinear least-squares fit.

Radicals were generated by photolysis of Cl_2 at wavelengths longer than the Pyrex cutoff, using $Cl_2/RCHO/O_2/N_2$ mixtures (where R = $(CH_3)_3C$ or $(CH_3)_2CH$):

$$Cl_2 + h\nu \rightarrow 2Cl \qquad (\text{for } \lambda > 280 \text{ nm}) \quad (3)$$

$$Cl + RCHO \rightarrow HCl + \text{radicals} \quad (4)$$

The concentration of Cl_2 was monitored using its absorption at 330 nm ($\sigma = 2.55 \times 10^{-19}$ cm^2 molecule^{-1}, from DeMore et al.[12]). Liquid reactants ($(CH_3)_3CCHO$ and $(CH_3)_2CHCHO$) were introduced into the reaction cell by passing a fraction of the diluent flow through the liquid, which was maintained at constant temperature (284 K for $(CH_3)_3CCHO$ and 273 K for $(CH_3)_2CHCHO$).

Acylperoxy- and carbonyl-substituted alkyl-peroxy radicals (hereafter, these are noted only as alkyl-peroxy radicals) were formed by adding an excess of oxygen to ensure rapid and stoichiometric conversion of the radicals that are formed via reaction 4 into peroxy radicals:

$$(CH_3)_3CC(O) + O_2 + M \rightarrow (CH_3)_3CC(O)O_2 + M \quad (5)$$

$$(CH_3)_2(CH_2)CCHO + O_2 + M \rightarrow (CH_3)_2(CH_2O_2)CCHO + M \quad (6)$$

$$(CH_3)_2CHC(O) + O_2 + M \rightarrow (CH_3)_2CHC(O)O_2 + M \quad (7)$$

$$CH_3(CH_2)CHCHO + O_2 + M \rightarrow CH_3(CH_2O_2)CHCHO + M \quad (8)$$

$$(CH_3)_2CCHO + O_2 + M \rightarrow (CH_3)_2CO_2CHO + M \quad (9)$$

Typical concentration ranges used were as follows: $[Cl_2] = (3-4) \times 10^{16}$ molecules cm^{-3} (Messer, 5% in N_2, purity >99.9%), $[(CH_3)_3CCHO] = (2.1-8.0) \times 10^{16}$ molecules cm^{-3} (Aldrich, 97%), $[(CH_3)_2CHCHO] = (1.8-6.5) \times 10^{16}$ molecules cm^{-3} (Aldrich, 99.5%), $[O_2] = 2.3 \times 10^{19}$ molecules cm^{-3} (Messer, 99.995%), and $[N_2] = 1 \times 10^{18}$ molecules cm^{-3} (Messer, 99.999%). No UV absorbing products were generated when gas mixtures that contained all reactants except Cl_2 were irradiated, which suggests that the present work is free from complications that are associated with the formation of absorbing radical species from the photolysis of the aldehydes.

2.2. Fourier Transform Infrared Smog Chamber System. Experiments were performed in a Pyrex reactor (capacity of 140 L) interfaced to a Mattson Sirus 100 FTIR spectrometer.[11] The optical path length of the infrared beam was 27 m. The reactor was surrounded by 22 fluorescent blacklamps (GE, model F15T8-BL), which were used to initiate the experiments photochemically, via the photolysis of Cl_2. The loss of $(CH_3)_3CCHO$ and $(CH_3)_2CHCHO$ and the formation of products were monitored by FTIR spectroscopy, using a spectral resolution of 0.25 cm^{-1}. IR spectra were derived from 32 co-added interferograms. Reference spectra were acquired by expanding known volumes of reference materials into the chamber. Products were identified and quantified by fitting reference spectra of the pure compounds to the observed product spectra, using integrated absorption features over the following wavenumber ranges (cm^{-1}): $(CH_3)_3CCHO$, 760−1900; $(CH_3)_2CHCHO$, 800−1800; $(CH_3)_3CC(O)Cl$, 760−1080; $(CH_3)_2CHC(O)Cl$, 660−1000; $(CH_3)_3CCl$, 1320−1410; $(CH_3)_2CHCl$, 860−1500; C_2H_4, 850−1050; C_2H_5Cl, 640−1350; C_6H_{12}, 1420−1480; CH_3OCHO, 1120−1800; and CO, 2050−2230.

All experiments were performed in 700 Torr of a N_2, or N_2/O_2, diluent at a temperature of 296 ± 2 K. Reagents were obtained from commercial sources at purities of >99% and were subjected to repeated freeze−pump−thaw cycling before use. In smog chamber experiments, it is important to check for an unwanted loss of reactants and products via photolysis, dark chemistry, and heterogeneous reactions. Control experiments were performed in which mixtures of reactants (except Cl_2) in N_2 were subjected to UV irradiation for 15 min and product mixtures obtained after the UV irradiation of reactant mixtures were allowed to stand in darkness in the chamber for 15 min. There was no observable loss of reactants or products, which

suggests that photolysis and heterogeneous reactions are not a significant complication in the present work. Unless otherwise stated, quoted uncertainties are two standard deviations from least-squares regressions.

3. Results

The results of investigations of the reactions of Cl atoms with $(CH_3)_3CCHO$, $(CH_3)_2CHCHO$, $(CH_3)_3CC(O)Cl$, $(CH_3)_2CHC(O)Cl$, $(CH_3)_3CCl$, and $(CH_3)_2CHCl$, of the reactions of $(CH_3)_3CC(O)$ and $(CH_3)_2CHC(O)$ with O_2 and Cl_2, and of the self-reaction of $(CH_3)_3CC(O)O_2$ and $(CH_3)_2CHC(O)O_2$ radicals, are reported below.

3.1. Relative Rate Study of the Reactions of Cl Atoms with $(CH_3)_3CCHO$ and $(CH_3)_2CHCHO$. The kinetics of reactions 1 and 2 were measured, relative to reactions 10 and 11, using the smog chamber system.

$$Cl + (CH_3)_3CCHO \rightarrow \text{products} \quad (1)$$

$$Cl + (CH_3)_2CHCHO \rightarrow \text{products} \quad (2)$$

$$Cl + C_2H_4 \rightarrow \text{products} \quad (10)$$

$$Cl + C_6H_{12}\ (\text{cyclohexane}) \rightarrow \text{products} \quad (11)$$

Reaction mixtures consisted of 21 mTorr of $(CH_3)_3CCHO$ or 16.3−21.7 mTorr of $(CH_3)_2CHCHO$, 104−132 mTorr of Cl_2, and either 4−7 mTorr of C_2H_4 or 7−19 mTorr of C_6H_{12}, in 700 Torr of N_2 diluent. Figure 1 shows the loss of $(CH_3)_3CCHO$ and $(CH_3)_2CHCHO$ versus loss of the reference compounds following the UV irradiation of $(CH_3)_3CCHO/Cl_2/\text{reference}/N_2$ and $(CH_3)_2CHCHO/Cl_2/\text{reference}/N_2$ mixtures. Linear least-squares analysis of the data in Figure 1 gives $k_1/k_{10} = 1.37 \pm 0.13$, $k_1/k_{11} = 0.302 \pm 0.025$, $k_2/k_{10} = 1.49 \pm 0.15$, and $k_2/k_{11} = 0.377 \pm 0.038$. Using $k_{10} = (9.29 \pm 0.93) \times 10^{-11}$ (from Wallington et al.[13]) and $k_{11} = (3.4 \pm 0.3) \times 10^{-10}$ (from Wallington et al.[14]), we derive $k_1 = (1.27 \pm 0.18) \times 10^{-10}$ and $(1.03 \pm 0.13) \times 10^{-10}$ and $k_2 = (1.38 \pm 0.14) \times 10^{-10}$ and $(1.28 \pm 0.18) \times 10^{-10}$ cm^3 molecule^{-1} s^{-1}. Consistent results were obtained in experiments conducted using the two different reference compounds. We choose to cite final values for k_1 and k_2, which are averages of the two determinations, together with error limits that encompass the extremes of the individual determinations. Hence, $k_1 = (1.15 \pm 0.30) \times 10^{-10}$ cm^3 molecule^{-1} s^{-1} and $k_2 = (1.33 \pm 0.25) \times 10^{-10}$ cm^3 molecule^{-1} s^{-1}.

3.2. Mechanism of the Reaction of Cl Atoms with $(CH_3)_3CCHO$. 3.2.1. Flash Photolysis Experiments. The reaction of Cl atoms with $(CH_3)_3CCHO$ leads to the formation of both acyl and alkyl radicals. In the presence of 710 Torr of O_2 at room temperature, the addition of O_2 occurs rapidly (>99% complete within 0.1 μs) and is essentially the sole fate of the acyl and alkyl radicals that are formed in reaction 1.[15,16] Hence, the conversion of Cl atoms into peroxy radicals is complete on a time scale that is essentially instantaneous, when compared to that of the observations (see Figure 2). The method used to determine the branching ratio ($\alpha_1 = k_{1a}/k_1$, corresponding to the channel forming acyl radicals) was based on the difference in acyl- and alkyl-peroxy radical absorptions in the 200−300 nm wavelength range.[15] Acyl-peroxy radicals, such as $(CH_3)_3CC(O)O_2$, have bimodal spectra with a strong absorption band centered at 207 nm ($\sigma(CH_3)_3CC(O)O_2 = 6.73 \times 10^{-18}$ cm^2 molecule^{-1}, from Tomas et al.[15]) and a weaker band near 240−250 nm. Alkyl-peroxy radicals, such as $(CH_3)_2(CH_2O_2)CCHO$, produced from reaction 1b have a single maximum absorption

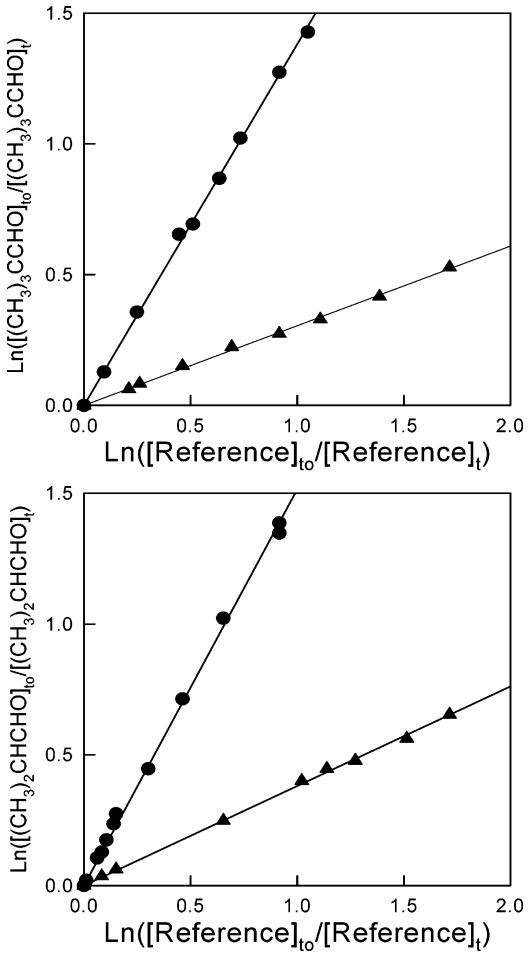

Figure 1. Loss of $(CH_3)_3CCHO$ (top panel) and $(CH_3)_2CHCHO$ (bottom panel) versus reference compounds (●) C_2h_4 and (▲) cyclohexane following exposure to Cl atoms in 700 Torr of N_2 diluent at 296 K.

centered near 240 nm. Decay traces were recorded at 207 and 240 nm. As a first approach, only the initial formation of the $(CH_3)_3CC(O)O_2$ radical was considered (such as that in the initiation of pivalaldehyde oxidation by Br atoms[9]); however, decay traces could not be simulated adequately with the chemical model that was presented in Table 1 (see Figure 2a). Consequently, formation of the $(CH_3)_2(CH_2O_2)CCHO$ radical was also considered. The sensitivity of the results to the $(CH_3)_2(CH_2O_2)CCHO$ radical reactions added in the chemical model (see Table 2) is discussed in Section 4.1. The total initial radical concentration was fixed and the proportion of $(CH_3)_3CC(O)O_2$ and $(CH_3)_2(CH_2O_2)CCHO$ was varied, to achieve the best fit to the experimental data at both 207 and 240 nm (see Figure 2b). The best fit was achieved with 12% initial formation of the $(CH_3)_2(CH_2O_2)CCHO$ radicals, yielding $\alpha_1 = k_{1a}/k_1 = 0.88 \pm 0.06$. It is possible that $(CH_3)_3CC(O)$ radicals that are formed in reaction 1a possess sufficient chemical activation to undergo prompt decomposition. Such prompt decomposition would lead to the formation of $(CH_3)_3CO_2$ radicals in the system. To investigate this possibility, simulations were performed in which $(CH_3)_2(CH_2O_2)CCHO$ radicals were replaced with $(CH_3)_3CO_2$ radicals. Experimental decays could not be simulated satisfactorily using a mechanism that involved the prompt decomposition of $(CH_3)_3CC(O)$ radicals.

3.2.2. FTIR Experiments. To determine the mechanism of the reaction of Cl atoms with $(CH_3)_3CCHO$, experiments were performed in which mixtures of 27−29 mTorr $(CH_3)_3CCHO$ and 0.038−2.81 Torr of Cl_2 in 700 Torr of N_2 diluent (including

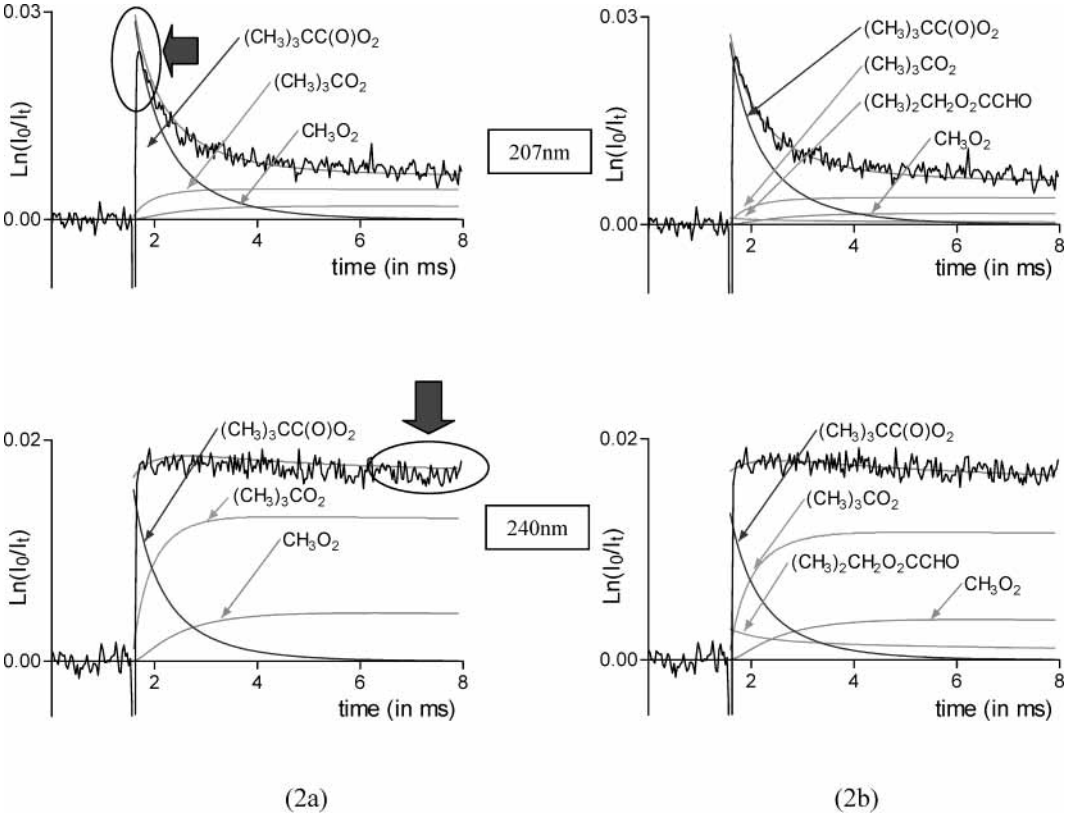

Figure 2. Decay traces at 207 and 240 nm obtained following irradiation of $Cl_2/(CH_3)_3CCHO/O_2/N_2$ mixtures. Solid lines are results of simulations assuming (a) either 100% conversion of Cl atoms into $(CH_3)_3CC(O)O_2$ radicals or (b) 88% conversion into $(CH_3)_3CC(O)O_2$ and 12% into $(CH_3)_2(CH_2O_2)CCHO$ radicals. Ellipses and arrows show the main changes in the simulations considering both cases.

TABLE 1: Chemical Mechanism Used in the Case of Initial Formation of the Pivaloylperoxy Radical Only at 298 K

reaction number	Chemical Reaction		rate constant (cm^3 molecule^{-1} s^{-1})	reference
	reactants	products		
23	$(CH_3)_3CC(O)O_2 + (CH_3)_3CC(O)O_2$	$\rightarrow 2(CH_3)_3CC(O)O + O_2$	$k_{23} = 1.45 \times 10^{-11}$	this work
24	$(CH_3)_3CC(O)O + M$	$\rightarrow (CH_3)_3C + CO_2 + M$	fast thermal decomposition	9
27	$(CH_3)_3C + O_2 + M$	$\rightarrow (CH_3)_3CO_2 + M$	$k_{27} > 1 \times 10^{-12}$	6
28	$(CH_3)_3CO_2 + (CH_3)_3CO_2$	$\rightarrow 2(CH_3)_3CO + O_2$	$k_{28} = 3 \times 10^{-17}$	6
29	$(CH_3)_3CO + M$	$\rightarrow (CH_3)_2CO + CH_3 + M$	$k_{29} = 800\ s^{-1}$	31
30	$CH_3 + O_2 + M$	$\rightarrow CH_3O_2 + M$	$k_{30} = 1.8 \times 10^{-12}$	31
31a	$CH_3O_2 + CH_3O_2$	$\rightarrow 2CH_3O + O_2$	$k_{31} = 3.5 \times 10^{-13}$	25
31b		$\rightarrow CH_2O + CH_3OH + O_2$	$k_{31a}/k_{31} = 0.37$	25
32	$CH_3O + O_2$	$\rightarrow CH_2O + HO_2$	$k_{32} = 1.92 \times 10^{-15}$	31
33	$HO_2 + HO_2$	$\rightarrow H_2O_2 + O_2$	$k_{33} = 3 \times 10^{-12}$	32
34	$(CH_3)_3CC(O)O_2 + (CH_3)_3CO_2$	$\rightarrow (CH_3)_3CC(O)O + (CH_3)_3CO + O_2$	$k_{34} = 1.25 \times 10^{-11}$	9
35a	$(CH_3)_3CC(O)O_2 + CH_3O_2$	$\rightarrow (CH_3)_3CC(O)O + CH_3O + O_2$	$k_{35} = 1.27 \times 10^{-11}$	24
35b		$\rightarrow (CH_3)_3CC(O)OH + CH_2O + O_2$	$k_{35a}/k_{35} = 0.7$	24
36a	$(CH_3)_3CC(O)O_2 + HO_2$	$\rightarrow (CH_3)_3CC(O)OOH + O_2$	$k_{36} = 4 \times 10^{-11} - 5 \times 10^{-11}$	see discussion
36b		$\rightarrow (CH_3)_3CC(O)OH + O_3$	$k_{36b}/k_{36} = 0.2$[a]	33
37a	$(CH_3)_3CO_2 + CH_3O_2$	$\rightarrow (CH_3)_3CO + CH_3O + O_2$	$k_{37} = 3.1 \times 10^{-15}$	26
37b		$\rightarrow (CH_3)_3COH + CH_2O + O_2$	$k_{37a}/k_{37} = 0.9$	26
38	$(CH_3)_3CO_2 + HO_2$	$\rightarrow (CH_3)_3COOH + O_2$	$k_{38} = 5.2 \times 10^{-12}$[a]	32
39	$CH_3O_2 + HO_2$	$\rightarrow CH_3OOH + O_2$	$k_{39} = 5.2 \times 10^{-12}$	32

[a] Rate constants unavailable in the literature, which were replaced by the rate constants of the corresponding acetyl- or methyl-peroxy radical reactions.

<0.5 ppm of O_2 impurity) were subjected to UV irradiation. Figure 3 shows typical IR spectra obtained before and after 1 s of UV irradiation of a mixture of 27 mTorr of $(CH_3)_3CCHO$ and 206 mTorr of Cl_2 in 700 Torr of N_2 diluent. Panel C in Figure 3 shows the result of subtracting features that are attributable to $(CH_3)_3CCHO$ from panel B in the same figure. Panels D, E, and F in Figure 3 show reference spectra of $(CH_3)_3CC(O)Cl$, $(CH_3)_3CCl$, and CO. It is clear from an inspection of Figure 3 that $(CH_3)_3CC(O)Cl$, $(CH_3)_3CCl$, and CO are major products. After subtraction of the features attributable to $(CH_3)_3CC(O)Cl$, $(CH_3)_3CCl$, and CO from panel C in the figure, small residual features were observed at 735, 951, 1124, 1742, and 1809 cm^{-1} that were presumably due to the formation of $(CH_2Cl)(CH_3)_2CCHO$.

Figure 4 shows a plot of the formation of $(CH_3)_3CCl$ versus CO following UV irradiation of the $(CH_3)_3CCHO/Cl_2/N_2$ mixtures. Filled symbols represent the observed data, and open symbols show the result of correcting the $(CH_3)_3CCl$ for secondary loss via reaction with Cl atoms (using kinetic data reported herein and algebraic expressions available in the literature[17]). The line through the data in Figure 4 is a least-squares fit to the corrected data, which gives a slope of 1.03 ±

TABLE 2: Reactions Added to the Chemical Mechanism Detailed in Table 1 to Account for the Initial Formation of the $(CH_3)_2(CH_2O_2)CCHO$ Radical

reaction number	Chemical Reaction: reactants	Chemical Reaction: products	rate constant (cm^3 molecule^{-1} s^{-1})	reference
40a	$2(CH_3)_2(CH_2O_2)CCHO$	$\rightarrow 2(CH_3)_2(CH_2O)CCHO + O_2$	$k_{40} = 4 \times 10^{-12}$	see discussion
40b		$\rightarrow (CH_3)_2(CH_2OH)CCHO + (CH_3)_2C(CHO)_2 + O_2$	$k_{40a}/k_{40} = 0.4$	34
41	$(CH_3)_2(CH_2O)CCHO + M$	$\rightarrow (CH_3)_2CCHO + CH_2O + M$	$k_{41} = 1.05 \times 10^{6}$ [a]	26
42	$(CH_3)_2CCHO + O_2 + M$	$\rightarrow (CH_3)_2CO_2CHO + M$	$k_{42} > 1 \times 10^{-12}$	6
43	$2(CH_3)_2CO_2CHO$	$\rightarrow 2(CH_3)_2COCHO + O_2$	$k_{43} = 2 \times 10^{-14}$	see discussion
44	$(CH_3)_2COCHO + M$	$\rightarrow (CH_3)_2CO + CHO + M$	instantaneous	see discussion
45	$CHO + O_2$	$\rightarrow HO_2 + CO$	$k_{45} = 5.5 \times 10^{-12}$	32
46a	$(CH_3)_2(CH_2O_2)CCHO + (CH_3)_3CC(O)O_2$	$\rightarrow (CH_3)_2(CH_2O)CCHO + (CH_3)_3CC(O)O + O_2$	$k_{46} = 1.4 \times 10^{-11}$ [b]	24
46b		$\rightarrow (CH_3)_2C(CHO)_2 + (CH_3)_3CC(O)OH$	$k_{46a}/k_{46} = 0.7$ [b]	24
47a	$(CH_3)_2(CH_2O_2)CCHO + (CH_3)_3CO_2$	$\rightarrow (CH_3)_2(CH_2O)CCHO + (CH_3)_3CO + O_2$	$k_{47} = 2.5 \times 10^{-14}$ [b]	23
47b		$\rightarrow (CH_3)_2(CHO)CCHO + (CH_3)_3COH + O_2$	$k_{47a}/k_{47} = 0.7$	23
48a	$(CH_3)_2(CH_2O_2)CCHO + CH_3O_2$	$\rightarrow (CH_3)_2(CH_2O)CCHO + CH_3O + O_2$	$k_{48} = 2.5 \times 10^{-12}$ [b]	23
48b		$\rightarrow (CH_3)_2C(CHO)_2 + CH_3OH + O_2$	$k_{48a}/k_{48} = 0.4$	23
48c		$\rightarrow (CH_3)_2(CH_2OH)CCHO + CH_2O + O_2$		
49	$(CH_3)_2(CH_2O_2)CCHO + HO_2$	$\rightarrow (CH_3)_2(CH_2OOH)CCHO + O_2$	$k_{49} = 1.42 \times 10^{-11}$ [a]	35
50a	$(CH_3)_2(CH_2O_2)CCHO + (CH_3)_2CO_2CHO$	$\rightarrow (CH_3)_2(CH_2O)CCHO + (CH_3)_2COCHO + O_2$	$k_{50} = 5 \times 10^{-13}$ [a,b]	23
50b		$\rightarrow (CH_3)_2C(CHO)_2 + (CH_3)_2C(OH)CHO + O_2$	$k_{50a}/k_{50} = 0.7$	23
51	$(CH_3)_2CO_2CHO + (CH_3)_3CC(O)O_2$	$\rightarrow (CH_3)_2COCHO + (CH_3)_3CC(O)O + O_2$	$k_{51} = 1.25 \times 10^{-11}$ [b]	24
52	$(CH_3)_2CO_2CHO + (CH_3)_3CO_2$	$\rightarrow (CH_3)_2COCHO + (CH_3)_3CO + O_2$	$k_{52} = 1 \times 10^{-15}$ [a]	23
53a	$(CH_3)_2CO_2CHO + CH_3O_2$	$\rightarrow (CH_3)_2COCHO + CH_3O + O_2$	$k_{53} = 1 \times 10^{-13}$ [a]	23
53b		$\rightarrow (CH_3)_2C(OH)CHO + CH_2O + O_2$	$k_{53a}/k_{53} = 0.7$	23
54	$(CH_3)_2CO_2CHO + HO_2$	$\rightarrow (CH_3)_2COOHCHO + O_2$	$k_{54} = 5.2 \times 10^{-12}$ [b]	32

[a] Rate constants unavailable in the literature, which were replaced by the rate constants of the corresponding neopentyl- or *tert*-butyl-peroxy radical reactions. [b] Considered to be similar to that of the corresponding acetyl- or methyl-peroxy radical reactions.

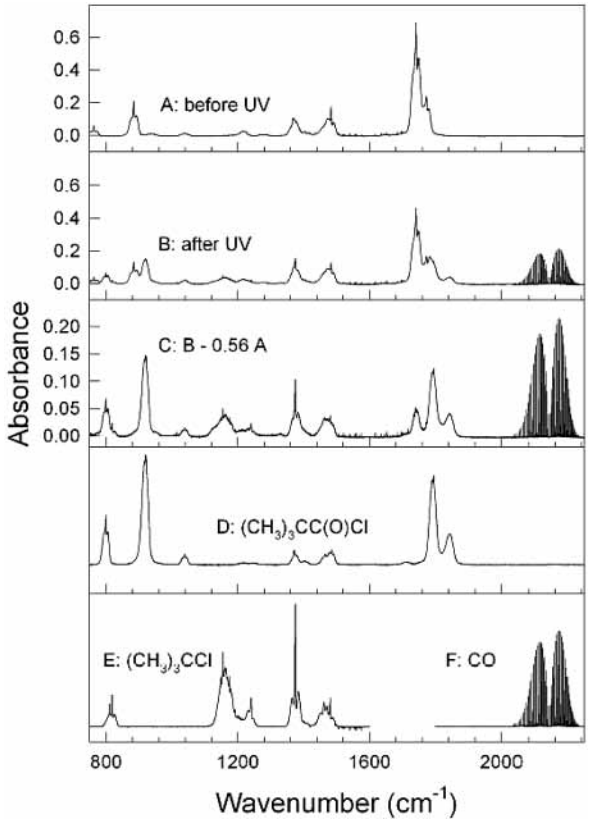

Figure 3. IR spectra obtained before (spectrum A) and after (spectrum B) a 1-s UV irradiation of a mixture of 27 mTorr $(CH_3)_3CCHO$ and 206 mTorr of Cl_2 in 700 Torr N_2 diluent. Spectrum C shows the result of subtracting features attributable to $(CH_3)_3CCHO$ from panel B. Spectra D, E, and F show reference spectra of $(CH_3)_3CC(O)Cl$, $(CH_3)_3CCl$, and CO, respectively.

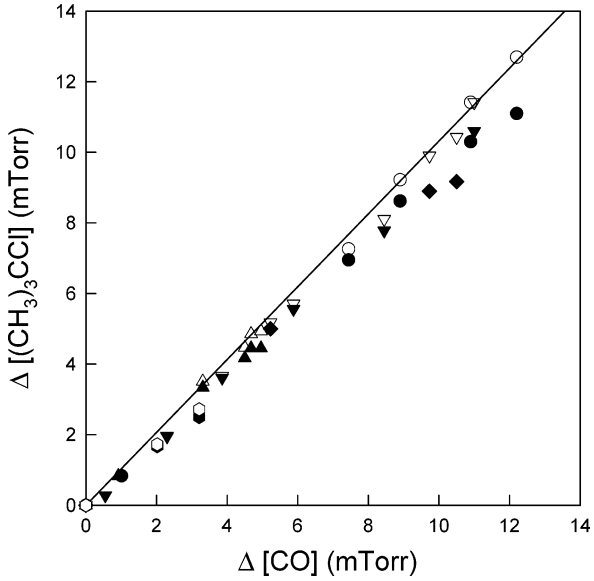

Figure 4. Formation of $(CH_3)_3CCl$ versus that of CO following UV irradiation of $(CH_3)_3CC(O)H/Cl_2$ mixtures in 700 Torr N_2 at 296 K. Filled symbols are observed data, whereas open symbols have been corrected for loss of $(CH_3)_3CCl$ via reaction with Cl atoms. Reaction mixtures consisted of 25 mTorr $(CH_3)_3CCHO$, 100 mTorr of Cl_2 (circles); 29 mTorr $(CH_3)_3CCHO$, 1010 mTorr of Cl_2 (triangles); 28 mTorr $(CH_3)_3CCHO$, 2030 mTorr of Cl_2 (inverted triangles); 27 mTorr $(CH_3)_3CCHO$, 206 mTorr of Cl_2 (diamonds); or 27 mTorr $(CH_3)_3CCHO$, 2810 mTorr of Cl_2 (hexagons).

0.07; the yields of $(CH_3)_3CCl$ and CO were indistinguishable. The inset in Figure 5 shows that the yield of $(CH_3)_3CC(O)Cl$ increased as $[Cl_2]$ increased. The simplest explanation of the experimental observations is that (i) reaction 1 proceeds via reactions 1a and 1b to give $(CH_3)_3CC(O)$ and $(CH_3)_2(CH_2)$-CCHO radicals, (ii) decomposition via CO elimination and reaction with Cl_2 are competing fates of $(CH_3)_3CC(O)$ radicals, and (iii) reaction with Cl_2 is the sole fate of $(CH_3)_3C$ radicals.

$$(CH_3)_3CC(O) + M \rightarrow (CH_3)_3C + CO + M \quad (12)$$

$$(CH_3)_3CC(O) + Cl_2 \rightarrow (CH_3)_3CC(O)Cl + Cl \quad (13)$$

$$(CH_3)_3C + Cl_2 \rightarrow (CH_3)_3CCl + Cl \quad (14)$$

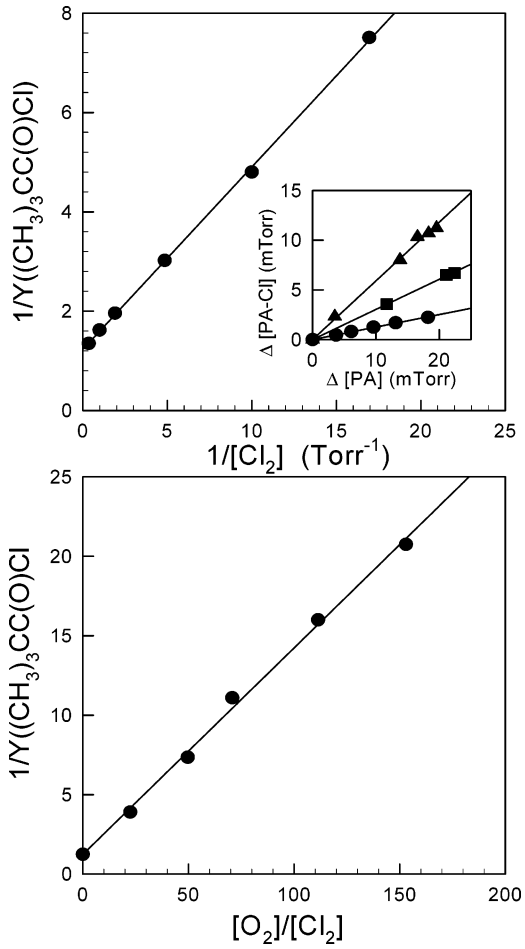

Figure 5. Top panel: reciprocal of the molar yield of $(CH_3)_3CC(O)Cl$ (Y) versus $1/[Cl_2]$, following UV irradiation of $(CH_3)_3CCHO/Cl_2/N_2$ mixtures. Bottom panel: reciprocal of the molar yield of $(CH_3)_3CC(O)Cl$ versus $[O_2]/[Cl_2]$ following UV irradiation of $(CH_3)_2CHCHO/Cl_2/N_2/O_2$ mixtures. Inset in the top panel shows a plot of the formation of $(CH_3)_3CC(O)Cl$ (=PA−Cl) versus the loss of $(CH_3)_3CCHO$ (=PA) following UV irradiation of mixtures of either 29 mTorr $(CH_3)_3CCHO$ and 1010 mTorr of Cl_2 (triangles), 27 mTorr $(CH_3)_3CCHO$ and 206 mTorr of Cl_2 (squares), or 27 mTorr $(CH_3)_3CCHO$ and 59 mTorr of Cl_2 (circles) in 700 Torr of N_2 diluent.

Assuming that reactions 12 and 13 are the sole fate of the $(CH_3)_3CC(O)$ radicals, the production rate of $(CH_3)_3CC(O)Cl$, $\Delta[(CH_3)_3CC(O)Cl]$, is thus related to the loss rate of $(CH_3)_3CCHO$, $\Delta[(CH_3)_3CCHO]$, as follows:

$$\Delta[(CH_3)_3CC(O)Cl] = \Delta[(CH_3)_3CCHO]\left(\frac{k_{1a}}{k_{1a}+k_{1b}}\right)\left(\frac{k_{13}[Cl_2]}{k_{12}+k_{13}[Cl_2]}\right)$$

The molar yield of $(CH_3)_3CC(O)Cl$, which is defined as $Y_{(CH_3)_3CC(O)Cl} \equiv \Delta[(CH_3)_3CC(O)Cl]/\Delta[(CH_3)_3CCHO]$, is given by

$$\frac{1}{Y_{(CH_3)_3CC(O)Cl}} = \left(\frac{k_{1a}+k_{1b}}{k_{1a}}\right)\left(\frac{k_{12}}{k_{13}[Cl_2]_0}\right) + \frac{k_{1a}+k_{1b}}{k_{1a}}$$

This indicates that a plot of $1/Y_{(CH_3)_3CC(O)Cl}$ versus $1/[Cl_2]_0$ should be linear, with a slope of $(k_{1a} + k_{1b})/k_{1a} \times (k_{12}/k_{13})$ and an intercept of $(k_{1a} + k_{1b})/k_{1a}$. The upper trace in Figure 5 shows a plot of $1/Y_{(CH_3)_3CC(O)Cl}$ versus $1/[Cl_2]_0$. Linear least-squares analysis gives an intercept $= (k_{1a} + k_{1b})/k_{1a} = 1.23 \pm 0.12$, from which we derive $\alpha_1 = k_{1a}/(k_{1a} + k_{1b}) = 0.81 \pm 0.08$, and a slope $= 0.38 \pm 0.03$ Torr, from which we derive $k_{12}/k_{13} = (1.00 \pm 0.13) \times 10^{16}$ cm^{-3} molecule. Reaction 12 is a collision-induced decomposition. By analogy to other radicals of a similar size, the kinetics of reaction 12 will be at, or close to, the high-pressure limit in 700 Torr. Accordingly, we assign units of s^{-1} to k_{12}.

3.3. Mechanism of the Reaction of Cl Atoms with $(CH_3)_2CHCHO$. 3.3.1. Flash Photolysis Experiments. The reaction of Cl atoms with isobutyraldehyde was investigated using the same method as that previously described for pivalaldehyde. Isobutyraldehyde has one H atom in the β-position from the carbonyl group and the formation of the $(CH_3)_2CCHO$ radical must be considered. In the presence of oxygen, $(CH_3)_2CHC(O)O_2$, $CH_3(CH_2O_2)CHCHO$, and $(CH_3)_2CO_2CHO$ may be formed according to reactions 7, 8, and 9, respectively. The UV absorption spectrum of the $(CH_3)_2CHC(O)O_2$ radical is reported elsewhere.[15] In the present work, we assume that the $CH_3(CH_2O_2)CHCHO$ radical has the same absorption spectrum as $(CH_3)_2(CH_2O_2)CCHO$ (see Section 4.1). Decay traces were recorded at 207 and 240 nm. As with the experiments that have involved pivalaldehyde, experimental traces could not be fit using a mechanism that only considered the formation of $(CH_3)_2CHC(O)O_2$ radicals (see Figure 6a). The introduction of $CH_3(CH_2O_2)CHCHO$ and $(CH_3)_2CO_2CHO$ radical chemistry (see Table 3) allowed us to fit the decay traces. The best fit to the decay traces at 207 and 240 nm (see Figure 6b) was achieved using the following branching ratios: $k_{2a}/k_2 = 0.85 \pm 0.05$, $k_{2b}/k_2 = 0.12 \pm 0.04$, and $k_{2c}/k_2 = 0.03 \pm 0.01$.

3.3.2. FTIR Experiments. To determine the fraction of the reaction of Cl atoms with $(CH_3)_2CHCHO$ that proceeds via attack on the aldehydic C−H, group experiments were performed using mixtures of 26−32 mTorr $(CH_3)_2CHCHO$ and 0.038−2.81 Torr of Cl_2 in 700 Torr of N_2 diluent. UV irradiation leads to the formation of $(CH_3)_2CHC(O)Cl$. The top panel in Figure 7 shows a plot of $1/Y_{(CH_3)_3CC(O)Cl}$ versus $1/[Cl_2]_0$. By analogy to the Cl + $(CH_3)_3CCHO$ reaction system, a linear least-squares fit to the data in Figure 7 gives an intercept of $(k_{2a} + k_{2b} + k_{2c})/k_{2a} = 1.18 \pm 0.12$ and a slope of $(k_{2a} + k_{2b} + k_{2c})/k_{2a} \times k_{15}/k_{16} = (1.33 \pm 0.15) \times 10^{-2}$ Torr. It follows that $\alpha_2 = k_{2a}/(k_{2a} + k_{2b} + k_{2c}) = 0.85 \pm 0.10$ and $k_{15}/k_{16} = (3.66 \pm 0.55) \times 10^{14}$ cm^{-3} molecule.

$$(CH_3)_2CHC(O) + M \rightarrow (CH_3)_2CH + CO + M \quad (15)$$

$$(CH_3)_2CHC(O) + Cl_2 \rightarrow (CH_3)_2CHC(O)Cl + Cl \quad (16)$$

3.4. Relative Rate Study of the Reactions of Cl Atoms with $(CH_3)_3CC(O)Cl$, $(CH_3)_2CHC(O)Cl$, $(CH_3)_3CCl$, and $(CH_3)_2CHCCl$. The kinetics of reactions 17−20 were measured relative to reactions 10, 21, and 22.

$$(CH_3)_3CC(O)Cl + Cl \rightarrow \text{products} \quad (17)$$

$$(CH_3)_2CHC(O)Cl + Cl \rightarrow \text{products} \quad (18)$$

$$(CH_3)_3CCl + Cl \rightarrow \text{products} \quad (19)$$

$$(CH_3)_2CHCl + Cl \rightarrow \text{products} \quad (20)$$

$$C_2H_5Cl + Cl \rightarrow \text{products} \quad (21)$$

$$CH_3OC(O)H + Cl \rightarrow \text{products} \quad (22)$$

Initial concentrations were either 10−11 mTorr $(CH_3)_3CC(O)Cl$, 13−15 mTorr $(CH_3)_2CHC(O)Cl$, 13−15 mTorr $(CH_3)_3CCl$, or 13−18 mTorr $(CH_3)_2CHCl$, 95−120 mTorr Cl_2, and either

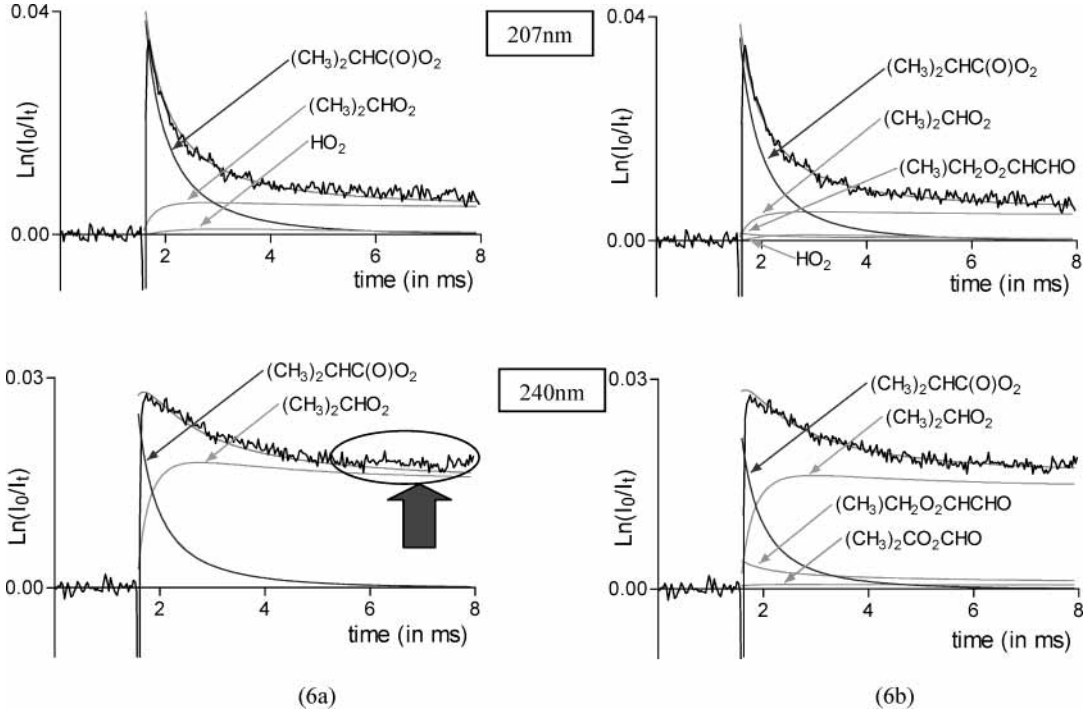

Figure 6. Decay traces at 207 and 240 nm obtained following UV irradiation of $Cl_2/(CH_3)_2CHCHO/O_2/N_2$ mixtures. Solid lines are results of simulations obtained by assuming either (a) 100% conversion of Cl atoms to $(CH_3)_2CHC(O)O_2$ radicals or (b) 85% conversion to $(CH_3)_2CHC(O)O_2$, 12% to $CH_3(CH_2O_2)CHCHO$, and 3% to $(CH_3)_2CO_2CHO$ radicals. Ellipse and arrow show the main changes in the simulations considering both cases.

6−15 mTorr C_2H_4, 11−18 mTorr C_2H_5Cl, or 9−13 mTorr $CH_3OC(O)H$ in 700 Torr of diluent (either N_2 or air). Measured rate constant ratios are given in Table 4. The data in Table 4 can be placed on an absolute basis, using values of $k_{10} = (9.29 \pm 0.93) \times 10^{-11}$ (from Wallington et al.[13]), $k_{21} = (8.04 \pm 0.57) \times 10^{-12}$ (from Wine and Semmes[18]), and $k_{22} = (1.40 \pm 0.10) \times 10^{-12}$ cm^3 molecule^{-1} s^{-1} (from Wallington et al. [19]) to give the results shown in Table 5. As observed in Table 5, indistinguishable values of k_{17}, k_{18}, k_{19}, and k_{20} were obtained using several different reference compounds, providing confidence in the results presented herein. We choose to quote final values, which are averages of the individual determinations, together with error limits which encompass the extremes of the individual determinations. Hence, $k_{17} = (6.86 \pm 1.50) \times 10^{-12}$, $k_{18} = (7.82 \pm 2.10) \times 10^{-12}$, $k_{19} = (1.27 \pm 0.21) \times 10^{-11}$, and $k_{20} = (2.01 \pm 0.49) \times 10^{-11}$ cm^3 molecule^{-1} s^{-1}.

3.5. Kinetics of the Reaction of $(CH_3)_3CC(O)$ Radicals with O_2 and Cl_2. The addition of O_2 to $(CH_3)_3CCHO/Cl_2/N_2$ reaction mixtures leads to a suppression of the yields of $(CH_3)_3CC(O)Cl$, $(CH_3)_3CCl$, and CO. This is reasonable because O_2 will compete for $(CH_3)_3CC(O)$ radicals via reaction 5. In the presence of high $[O_2]$, the decomposition channel reaction 12 becomes a negligible loss mechanism for $(CH_3)_3CC(O)$ radicals and the competition between reactions 13 and 5 can be studied.

The production rate of $(CH_3)_3CC(O)Cl$ ($\Delta[(CH_3)_3CC(O)Cl]$) is thus related to the loss rate of $(CH_3)_3CCHO$ ($\Delta[(CH_3)_3CCHO]$) as follows:

$$\Delta[(CH_3)_3CC(O)Cl] = \Delta[(CH_3)_3CCHO] \times \frac{k_{1a}}{k_{1a}+k_{1b}} \times \frac{k_{13}[Cl_2]}{k_{13}[Cl_2]+k_5[O_2]}$$

The molar yield of $(CH_3)_3CC(O)Cl$ ($Y_{(CH_3)_3CC(O)Cl} \equiv \Delta[(CH_3)_3CC(O)Cl]/\Delta[(CH_3)_3CCHO]$) is given by

$$\frac{1}{Y_{(CH_3)_3CC(O)Cl}} = \frac{k_{1a}+k_{1b}}{k_{1a}} \cdot \frac{k_5}{k_{13}} \cdot \frac{[O_2]}{[Cl_2]} + \frac{k_{1a}+k_{1b}}{k_{1a}}$$

The bottom panel in Figure 5 shows a plot of $1/Y_{(CH_3)_3CC(O)Cl}$ versus the $[O_2]/[Cl_2]$ concentration ratio obtained in the presence of 100 Torr of O_2 with varying amounts of $[Cl_2]$. Linear least-squares analysis of the data in Figure 5 gives a slope of $(k_{1a} + k_{1b})/k_{1a} \times (k_5/k_{13}) = 0.130 \pm 0.011$ which can be combined with the value of $(k_{1a} + k_{1b})/k_{1a} = 1.23 \pm 0.12$ determined in Section 3.2.2 to give $k_5/k_{13} = 0.106 \pm 0.013$. This result is consistent with the analogous behavior of $CH_3C(O)$ and $C_6H_5C(O)$ radicals, which react with O_2 at rate constants that are approximately an order of magnitude lower than the corresponding reactions with Cl_2 in 700 Torr of N_2 diluent.[20] On the baiss of the literature data for $CH_3C(O)$ and $C_6H_5C(O)$ radicals,[20,21] it seems reasonable to assume that k_{13} is of the order of 10^{-11} cm^3 molecule^{-1} s^{-1} at a total pressure of 700 Torr, and hence k_5 is of the order of 10^{-12} cm^3 molecule^{-1} s^{-1}. From the value of $k_{12}/k_{13} = (1.00 \pm 0.13) \times 10^{16}$ cm^{-3} molecule determined in Section 3.2.2, we conclude that k_{12} is $\sim 1 \times 10^5$ s^{-1}.

The measurements of $k_5/k_{13} = 0.106 \pm 0.013$ and $k_{12}/k_{13} = (1.00 \pm 0.13) \times 10^{16}$ cm^3 molecule^{-1} can be combined to give $k_5/k_{12} = (1.06 \pm 0.19) \times 10^{-17}$ cm^{-3} molecule. In 1 atm of air at 296 K, $[O_2] = 5.2 \times 10^{18}$ cm^{-3} and 98.2% of $(CH_3)_3CC(O)$ radicals will add O_2 whereas 1.8% will undergo decomposition via CO elimination. In the present determination of k_5/k_{12}, the temperature was 296 K and the total pressure was 700 Torr. These conditions are representative of the lowest portion of the Earth's atmosphere. With increasing altitude, the temperature, total pressure, and oxygen partial pressure all decrease. The absolute rates of reaction 12 and 13 will both decrease with increasing altitude. However, as discussed elsewhere[22] the sensitivity of the unimolecular decomposition reaction 12 will

TABLE 3: Chemical Mechanism Used to Simulate the Reactions Arising from the $Cl_2/(CH_3)_2CHCHO/N_2/O_2$ Mixture at 298 K

reaction number	Chemical Reaction: reactants	products	rate constant (cm^3 $molecule^{-1}$ s^{-1})	reference
25	$2(CH_3)_2CHC(O)O_2$	$\rightarrow 2(CH_3)_2CHC(O)O + O_2$	$k_{25} = 1.44 \times 10^{-11}$	this work
26	$(CH_3)_2CHC(O)O + M$	$\rightarrow (CH_3)_2CH + CO_2 + M$	fast thermal decomposition	9
55	$(CH_3)_2CH + O_2 + M$	$\rightarrow (CH_3)_2CHO_2 + M$	$k_{55} = 1.1 \times 10^{-11}$	32
56a	$2(CH_3)_2CHO_2$	$\rightarrow 2(CH_3)_2CHO + O_2$	$k_{56} = 1 \times 10^{-15}$	26
56b		$\rightarrow (CH_3)_2CO + (CH_3)_2CHOH + O_2$	$k_{56a}/k_{56} = 0.56$	26
57	$(CH_3)_2CHO + O_2$	$\rightarrow (CH_3)_2CO + HO_2$	$k_{57} = 7.7 \times 10^{-15}$	31
33	$HO_2 + HO_2$	$\rightarrow H_2O_2 + O_2$	$k_{33} = 3 \times 10^{-12}$	32
58a	$(CH_3)_2CHC(O)O_2 + (CH_3)_2CHO_2$	$\rightarrow (CH_3)_2CHC(O)O + (CH_3)_2CHO + O_2$	$k_{58} = 1 \times 10^{-11}$	9
58b		$\rightarrow (CH_3)_2CHC(O)OH + (CH_3)_2CO + O_2$	$k_{58a}/k_{58} = 0.35$	9
59a	$(CH_3)_2CHC(O)O_2 + HO_2$	$\rightarrow (CH_3)_2CHC(O)OOH + O_2$	$k_{59} = 2 \times 10^{-11} - 3 \times 10^{-11}$	see discussion
59b		$\rightarrow (CH_3)_2CHC(O)OH + O_3$	$k_{59b}/k_{59} = 0.2$[a]	33
60	$(CH_3)_2CHO_2 + HO_2$	$\rightarrow (CH_3)_2CHOOH + O_2$	$k_{60} = 5.2 \times 10^{-12}$ [a]	26
61a	$2(CH_3)CH_2O_2CHCHO$	$\rightarrow 2(CH_3)(CH_2O)CCHO + O_2$	$k_{61} = 5 \times 10^{-12}$	See discussion
61b		$\rightarrow (CH_3)(CH_2OH)CHCHO + (CH_3)CH(CHO)_2 + O_2$	$k_{61a}/k_{61} = 0.4$[b]	26
62	$(CH_3)CH_2OCHCHO + M$	$\rightarrow CH_3CHCHO + CH_2O + M$	$k_{62} = 1.05 \times 10^{6}$ [b]	10
63	$CH_3CHCHO + O_2 + M$	$\rightarrow CH_3CHO_2CHO + M$	$k_{63} = 1.1 \times 10^{-11}$ [b]	31
64a	$2\ CH_3CHO_2CHO$	$\rightarrow 2CH_3CHOCHO + O_2$	$k_{64} = 1 \times 10^{-14}$ [b]	See discussion
64b		$\rightarrow CH_3C(O)CHO + CH_3CH(OH)CHO + O_2$	$k_{64a}/k_{64} = 0.56$[b]	See discussion
65a	$(CH_3)CH_2O_2CHCHO + (CH_3)_2CHC(O)O_2$	$\rightarrow (CH_3)CH_2OCCHO + (CH_3)_2CHC(O)O + O_2$	$k_{65} = 1.4 \times 10^{-11}$ [b]	23
65b		$\rightarrow (CH_3)_2C(CHO)_2 + (CH_3)_3CC(O)OH$	$k_{65a}/k_{65} = 0.7$[b]	23
66a	$(CH_3)CH_2O_2CHCHO + (CH_3)_2CHO_2$	$\rightarrow (CH_3)CH_2OCCHO + (CH_3)_2CHO + O_2$	$k_{66} = 1.4 \times 10^{-13}$ [a]	23
66b		$\rightarrow$ molecular products	$k_{66a}/k_{66} = 0.5$[a]	23
67	$(CH_3)CH_2O_2CHCHO + HO_2$	$\rightarrow (CH_3)_2CH_2OOHCCHO + O_2$	$k_{67} = 1.42 \times 10^{-11}$ [b]	35
68a	$(CH_3)CH_2O_2CHCHO + CH_3CHO_2CHO$	$\rightarrow (CH_3)_2(CH_2O)CCHO + (CH_3)_2COCHO + O_2$	$k_{68} = 1.4 \times 10^{-13}$ [b]	23
68b		$\rightarrow$ molecular products	$k_{68a}/k_{68} = 0.5$[b]	23
69a	$CH_3CHO_2CHO + (CH_3)_2CHC(O)O_2$	$\rightarrow CH_3CHOCHO + (CH_3)_2CHC(O)O + O_2$	$k_{69} = 1 \times 10^{-11}$ [b]	9
69b		$\rightarrow CH_3C(O)CHO + (CH_3)_2CHC(O)OH + O_2$	$k_{69a}/k_{69} = 0.35$[b]	9
70a	$CH_3CHO_2CHO + (CH_3)_2CHO_2$	$\rightarrow (CH_3)_2COCHO + (CH_3)_3CO + O_2$	$k_{70} = 6 \times 10^{-15}$ [b]	23
70b		$\rightarrow$ molecular products	$k_{70a}/k_{70} = 0.56$[b]	23
43	$2(CH_3)_2CO_2CHO$	$\rightarrow 2(CH_3)_2COCHO + O_2$	$k_{43} = 1 \times 10^{-14}$	see discussion
71	$(CH_3)_2CO_2CHO + (CH_3)_2CHC(O)O_2$	$\rightarrow (CH_3)_2COCHO + (CH_3)_2CHC(O)O + O_2$	$k_{71} = 1.25 \times 10^{-11}$ [a]	9
72a	$(CH_3)_2CO_2CHO + (CH_3)_2CHO_2$	$\rightarrow (CH_3)_2COCHO + (CH_3)_2CHO + O_2$	$k_{72} = 6 \times 10^{-15}$ [b]	23
72b		$\rightarrow (CH_3)_2COHCHO + (CH_3)_2CO + O_2$	$k_{72a}/k_{72} = 0.7$[b]	23
73a	$(CH_3)_2CO_2CHO + (CH_3)CH_2O_2CHCHO$	$\rightarrow (CH_3)_2COCHO + (CH_3)CH_2OCHCHO + O_2$	$k_{73} = 5 \times 10^{-13}$ [b]	23
73b		$\rightarrow (CH_3)_2COHCHO + (CH_3)CH(CHO)_2 + O_2$	$k_{73a}/k_{73} = 0.7$[b]	23
74a	$(CH_3)_2CO_2CHO + CH_3CHO_2CHO$	$\rightarrow (CH_3)_2CO_2CHO + CH_3CHO_2CHO + O_2$	$k_{74} = 1 \times 10^{-14}$ [b]	23
74b		$\rightarrow (CH_3)_2COHCHO + CH_3C(O)CHO + O_2$	$k_{74a}/k_{74} = 0.7$[b]	23

[a] Assumed the same as in the corresponding acetyl- or methyl-peroxy radical reactions. [b] Considered to be similar to that of the corresponding isopropyl-, neopentyl-, or *tert*-butyl-peroxy radical reactions.

TABLE 4: Measured Rate Constant Ratio ($k_{reactant}/k_{reference}$) for Reactions with Cl Atoms in 700 Torr of N_2, or Air, at 296 K for Various References

reactant	$k_{reactant}/k_{reference}$: C_6H_{12}	C_2H_4	C_2H_5Cl	CH_3OCHO
$(CH_3)_3CCHO$	0.302 ± 0.025	1.37 ± 0.13		
$(CH_3)_2CHCHO$	0.377 ± 0.038	1.49 ± 0.15		
$(CH_3)_3CC(O)Cl$		0.077 ± 0.010	0.784 ± 0.057	5.06 ± 0.45
$(CH_3)_2CHC(O)Cl$		0.093 ± 0.010	0.871 ± 0.080	5.58 ± 0.56
$(CH_3)_3CCl$		0.141 ± 0.012	1.53 ± 0.13	
$(CH_3)_2CHCl$		0.235 ± 0.024	2.28 ± 0.23	

TABLE 5: Measured Rate Constant for Reactions with Cl Atoms in 700 Torr of N_2, or Air, at 296 K for Various References

reactant	Measured Rate Constant (cm^3 $molecule^{-1}$ s^{-1}): C_6H_{12}	C_2H_4	C_2H_5Cl	CH_3OCHO	mean
$(CH_3)_3CCHO$	$(1.03 \pm 0.12) \times 10^{-10}$	$(1.27 \pm 0.18) \times 10^{-10}$			$(1.15 \pm 0.30) \times 10^{-10}$
$(CH_3)_2CHCHO$	$(1.28 \pm 0.17) \times 10^{-10}$	$(1.38 \pm 0.20) \times 10^{-10}$			$(1.33 \pm 0.25) \times 10^{-10}$
$(CH_3)_3CC(O)Cl$		$(7.19 \pm 1.17) \times 10^{-12}$	$(6.30 \pm 0.64) \times 10^{-12}$	$(7.08 \pm 0.81) \times 10^{-12}$	$(6.86 \pm 1.50) \times 10^{-12}$
$(CH_3)_2CHC(O)Cl$		$(8.65 \pm 1.27) \times 10^{-12}$	$(7.00 \pm 0.81) \times 10^{-12}$	$(7.81 \pm 0.96) \times 10^{-12}$	$(7.82 \pm 2.10) \times 10^{-12}$
$(CH_3)_3CCl$		$(1.31 \pm 0.17) \times 10^{-11}$	$(1.23 \pm 0.14) \times 10^{-11}$		$(1.27 \pm 0.21) \times 10^{-11}$
$(CH_3)_2CHCCl$		$(2.19 \pm 0.31) \times 10^{-11}$	$(1.83 \pm 0.23) \times 10^{-11}$		$(2.01 \pm 0.49) \times 10^{-11}$

dominate and the ratio $k_{12}/(k_{13} \times [O_2])$ will decrease with altitude. We conclude that in the atmosphere >98% of $(CH_3)_3CC(O)$ radicals will add O_2 to form the corresponding peroxy radical.

3.6. Kinetics of the Reaction of $(CH_3)_2CHC(O)$ Radicals with O_2 and Cl_2. The addition of O_2 to $(CH_3)_2CHC(O)H/Cl_2/N_2$ reaction mixtures resulted in a suppression of the yields of $(CH_3)_2CHC(O)Cl$, $(CH_3)_2CHCl$, and CO. This is reasonable, because O_2 will compete for $(CH_3)_2CHC(O)$ radicals via reaction 7. In the presence of high $[O_2]$, the decomposition channel reaction 15 becomes a negligible loss mechanism for $(CH_3)_2CHC(O)$ radicals and the competition between reactions 16 and 7 can be studied. The bottom panel in Figure 7 shows a plot of $1/Y_{(CH_3)_2CHC(O)Cl}$ versus $[O_2]/[Cl_2]$ for experiments performed in the presence of 100 Torr of O_2 with varying amounts of $[Cl_2]$. By analogy to the reactions of $(CH_3)_3CC(O)$ with O_2 and Cl_2,

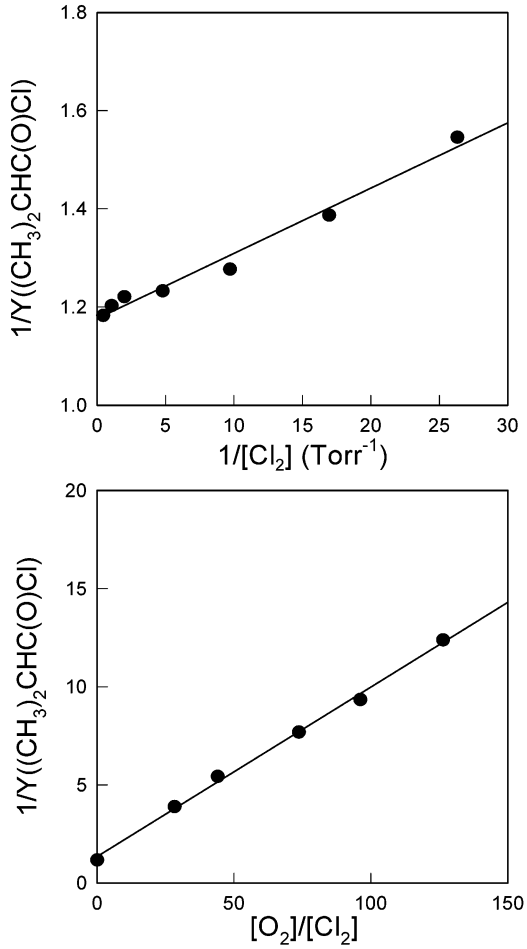

Figure 7. Top panel: reciprocal of the molar yield of $(CH_3)_2CHC(O)Cl$ ($Y_{(CH_3)_2CHC(O)Cl}$) versus $1/[Cl_2]$ following UV irradiation of $(CH_3)_2CHCHO/Cl_2/N_2$ mixtures. Bottom panel: reciprocal of the molar yield of $(CH_3)_2CHC(O)Cl$ ($Y_{(CH_3)_2CHC(O)Cl}$) versus $[O_2]/[Cl_2]$, following UV irradiation of $(CH_3)_2CHCHO/Cl_2/N_2/O_2$ mixtures.

linear least-squares analysis gives a slope $= (k_{2a} + k_{2b} + k_{2c})/[k_{2a} \times (k_7/k_{16})] = (8.63 \pm 1.06) \times 10^{-2}$. Using the value of $(k_{2a} + k_{2b} + k_{2c})/k_{2a} = 1.18 \pm 0.12$ from Section 3.3.2 gives $k_7/k_{16} = (7.31 \pm 1.19) \times 10^{-2}$. As described previously, this result is consistent with the analogous behavior of $CH_3C(O)$ and $C_6H_5C(O)$ radicals. Using the same arguments as those presented in Section 3.5, it seems reasonable to assume that k_{16} is of the order of 10^{-11} cm^3 molecule^{-1} s^{-1} and k_7 is of the order of 10^{-12} cm^3 molecule^{-1} s^{-1}. From the value of $k_{15}/k_{16} = (3.66 \pm 0.55) \times 10^{14}$ cm^{-3} molecule determined in Section 3.3.2, we conclude that $k_{15} \approx 4 \times 10^3$ s^{-1}.

Combining $k_{15}/k_{16} = (3.66 \pm 0.55) \times 10^{14}$ cm^{-3} molecule with $k_7/k_{16} = (7.31 \pm 1.19) \times 10^{-2}$ gives $k_7/k_{15} = (2.0 \pm 0.5) \times 10^{-16}$ cm^{-3} molecule. In 1 atm of air at 296 K, $[O_2] = 5.2 \times 10^{18}$ cm^{-3}. Using the logic presented in Section 3.5, it follows that, in the atmosphere, >99.8% of $(CH_3)_2CHC(O)$ will add O_2 and <0.2% will undergo decomposition.

3.7. Kinetics of the $(CH_3)_3CC(O)O_2$ and $(CH_3)_2CHC(O)O_2$ Self-Reactions. The self-reactions of $(CH_3)_3CC(O)O_2$ and $(CH_3)_2CHC(O)O_2$ radicals initiate a complex series of reactions, which are detailed in Tables 1, 2, and 3.

$$(CH_3)_3CC(O)O_2 + (CH_3)_3CC(O)O_2 \rightarrow 2(CH_3)_3CC(O)O + O_2 \quad (23)$$

$$(CH_3)_3CC(O)O + M \rightarrow (CH_3)_3C + CO_2 + M \quad (24)$$

$$(CH_3)_2CHC(O)O_2 + (CH_3)_2CHC(O)O_2 \rightarrow 2(CH_3)_2CHC(O)O + O_2 \quad (25)$$

$$(CH_3)_2CHC(O)O + M \rightarrow (CH_3)_2CH + CO_2 + M \quad (26)$$

Decay traces were recorded at two wavelengths, 207 and 240 nm, which corresponded to the maximum absorption of $(CH_3)_3CC(O)O_2$ (or $(CH_3)_2CHC(O)O_2$, in the case of isobutyraldehyde) and $(CH_3)_3CO_2$ (or $(CH_3)_2CHO_2$) radicals, respectively. Most kinetic information was derived from the traces at 207 nm, where concentration and absorption cross section of acylperoxy radical dominate all other absorbing species, as shown in the upper traces in Figures 2 and 6. Traces at 240 nm are quite flat, because $(CH_3)_3CC(O)O_2$ (or $(CH_3)_2CHC(O)O_2$) radicals are converted mainly to $(CH_3)_3CO_2$ (or $(CH_3)_2CHO_2$) radicals, which present a rather slow self-reaction. Moreover, $(CH_3)_3CC(O)O_2$ and $(CH_3)_3CO_2$ have a similar absorption cross section at 240 nm; hence, the traces are essentially flat, as shown in the lower trace in Figure 2. Although the 240 nm traces do not provide much kinetic information, they do provide mechanistic information.

Decay traces were simulated by considering the complete chemical mechanism (see Tables 1, 2, and 3). The rate constants of the $(CH_3)_3CC(O)O_2$ and $(CH_3)_2CHC(O)O_2$ radical self-reactions were adjusted to fit the decay traces. The rate constants for cross reactions between all RO_2 and $RC(O)O_2$ radicals were estimated from previous structure activity relationships (SARs) on peroxy radical cross reactions.[23,24] Ten determinations of k_{23} and six determinations of k_{25} were performed, resulting in the following rate constants at room temperature: $k_{23} = (1.45 \pm 0.07) \times 10^{-11}$ and $k_{25} = (1.44 \pm 0.10) \times 10^{-11}$ cm^3 molecule^{-1} s^{-1}.

4. Discussion

4.1. Accuracy of Results from Flash Photolysis Experiments. Several factors influence the accuracy of the results obtained in flash photolysis experiments. The chemistry associated with peroxy radical reactions is very complicated (see Tables 1, 2, and 3). The chemical mechanisms used in the kinetic analysis were taken from the literature.[9] To quantify the sensitivity of the branching ratios α_1 and α_2 to the parameters used for analysis, a systematic analysis of the propagation of errors was performed, as described previously.[10] Determination of the branching ratios α_1 and α_2 is dependent on the calibration of the total initial radical concentration and on the absorption cross sections of $(CH_3)_3CC(O)O_2$ and $(CH_3)_2(CH_2O_2)CCHO$ radicals for the pivalaldehyde system ($(CH_3)_2CHC(O)O_2$, $CH_3(CH_2O_2)CHCHO$, and $(CH_3)_2CO_2CHO$ radicals for the isobutyraldehyde system).

Calibration of the total radical concentration was achieved by replacing the aldehyde by methane (CH_4), keeping all other conditions constant. In the presence of CH_4, the Cl atoms are converted into CH_3O_2 radicals, the absorption spectrum of which is well established.[25] Uncertainties associated with the $(CH_3)_3CC(O)O_2$ and $(CH_3)_2CHC(O)O_2$ cross sections are estimated to be 20%,[15] resulting in approximately 20% uncertainty in the self-reaction rate constants k_{23} and k_{25} and ~18% uncertainty in the α_1 and α_2 values. Uncertainties on the $(CH_3)_2(CH_2O_2)CCHO$, $CH_3(CH_2O_2)CHCHO$, and $(CH_3)_2CO_2CHO$ cross sections were estimated at 30%, with their values being extrapolated from that of the following methylated peroxy radicals: $(CH_3)_2(CH_2O_2)CCH_3$, $CH_3(CH_2O_2)CHCH_3$, and $(CH_3)_2CO_2CH_3$.[26] The only examples of the influence of a carbonyl group on peroxy radical absorption reported in the literature are when the

carbonyl is positioned α or β from the peroxy group (i.e., for $CH_3C(O)O_2$ and $CH_3C(O)CH_2O_2$), which leads to the presence of two absorption bands.[27] In the case of $(CH_3)_2(CH_2O_2)CCHO$, $CH_3(CH_2O_2)CHCHO$, and $(CH_3)_2CO_2CHO$, the carbonyl group is in the β- or γ-position, i.e., remote from the peroxy chromophore, and it seems reasonable to assume that its influence will be small. To test this assumption, experiments were performed in which pivalaldehyde and isobutyraldehyde were replaced by their corresponding ketones: 1,1,1-trimethylacetone and 3-methyl,2-butanone (3MB). The observed total absorption, corresponding to the absorption of the two (or three for 3MB) peroxy radicals that are expected to be formed, consisted of only one wide band that was centered at ∼240 nm. No evidence for an additional absorption band at ∼210 nm was observed, which indicated that the presence of a γ-carbonyl group has little (or no) effect on the usual alkyl peroxy band.

Even if there are some uncertainties in the mechanisms used to simulate experimental traces, note that these complete mechanisms were not required to extract the value of the branching ratios α_1 and α_2. The simulations at both 207 and 240 nm just provides a good indication of the validity of the reaction mechanisms and, thus, allowed us to further propose acylperoxy self-reactions rate constant values, to be compared to those already reported in the literature.[9] The unknown rate constants, particularly those of the peroxy cross reactions, were derived either using the geometric average of the self-reaction rate constants[23] in the case of alkylperoxy radicals or using a similar value as that of the acetylperoxy self-reaction in the case of acylperoxy radicals, as recommended by Villenave and Lesclaux.[24]

For the pivalaldehyde system, a variation of 20% in the $(CH_3)_3CC(O)O_2$ self-reaction rate constant results in a variation of 19% in the value of α_1. Variation of the $(CH_3)_2(CH_2O_2)$-CCHO self-reaction rate constant by a factor of 2 results in a variation of only 5% in α. Allowing for an uncertainty of 50% in the rate constant for the cross reaction $(CH_3)_3CC(O)O_2 + (CH_3)_2(CH_2O_2)CCHO$ results in an uncertainty of 14% in the value of α_1. Using values of $k((CH_3)_3CC(O)O_2 + HO_2)$ from 1×10^{-11} to 5×10^{-11} cm^3 molecule^{-1} s^{-1} did not change the value of the branching ratio, because of the small quantities of HO_2 present in the system. Combining the uncertainties described above we estimate a global systematic uncertainty of 24% in α_1.

A similar analysis was conducted in the case of isobutyraldehyde, which yielded a global systematic uncertainty of 25% in the value of α_2.

4.2. Reactions of Cl Atoms with $(CH_3)_3CCHO$ and $(CH_3)_2CHCHO$. Rate constants for reactions of Cl atoms with pivalaldehyde and isobutyraldehyde determined in the present work are in agreement, within the combined experimental uncertainties, with previous relative rate studies by Thévenet et al.[28] ($k_1 = (1.6 \pm 0.3) \times 10^{-10}$ and $k_2 = (1.7 \pm 0.3) \times 10^{-10}$) and Ullerstam et al.[29] ($k_1 = (1.2 \pm 0.2) \times 10^{-10}$ and $k_2 = (1.5 \pm 0.3) \times 10^{-10}$ cm^3 molecule^{-1} s^{-1}). Both previous studies noted that the reactions proceed with rates that are similar to the gas kinetic limit. After comparing the reactivity of the aldehydes and their alkane analogues (e.g., pivalaldehyde and 2,2-dimethylpropane), it was concluded that the aldehydic H atom adds little, in terms of the overall reactivity of the molecule.[29] Thévenet et al.[28] further concluded that abstraction of the aldehydic H-atom is of minor importance. Our study shows that this conclusion is incorrect; abstraction of the aldehydic H atom is the major reaction channel.

The present study is the first investigation of the mechanism of the reactions of Cl atoms with pivalaldehyde and isobutyraldehyde. We show that these reactions proceed predominantly (80%−90%) by abstraction of the aldehydic H atom. This result is consistent with previous reports,[7,8] that the reaction of Cl atoms with acetaldehyde proceeds predominantly (>99% for Niki et al.[8] and >95% for Bartels et al.[7]) via abstraction of the aldehydic H atom.

4.3. Thermal Decomposition of $(CH_3)_3CC(O)$ and $(CH_3)_2CHC(O)$ Radicals. The rates of decomposition of $(CH_3)_3CC(O)$ and $(CH_3)_2CHC(O)$ were determined at room temperature and atmospheric pressure. For $(CH_3)_3CC(O)$, our estimate of $k_{12} = 1 \times 10^5$ s^{-1} can be compared to values of $k_{12} = 3.0 \times 10^5$ and 1.3×10^5 s^{-1} that have been reported by Jagiella et al.[16] and Tomas et al.[15] at 298 K in 1 atm of air. For $(CH_3)_2CHC(O)$, our estimate of $k_{15} = 4 \times 10^3$ s^{-1} can be compared to previous estimates of $k_{15} = 1.2 \times 10^4$ and 7.1×10^3 s^{-1} that have been reported by Jagiella et al.[16] and Tomas et al.[15] at 298 K in 1 atm of air. In the present work, the rate of decomposition of the RC(O) radical was measured relative to its reaction with Cl_2. In the studies by Jagiella et al.[16] and Tomas et al.,[15] the rate of decomposition of the RC(O) radical was measured, relative to its reaction with O_2. There is no kinetic data concerning the reactions of $(CH_3)_3CC(O)$ and $(CH_3)_2CHC(O)$ with either Cl_2 or O_2. The relative rate data in all three studies were placed, on an absolute basis, by assuming that the reference reactions proceed with rates similar to those of analogous acyl radicals whose kinetics have been studied. Given the indirect methods that have been used, the fact that the results agree to within a factor of 3 can be considered reasonable agreement. The factor of ∼2 difference in results from Jagiella et al.[16] and Tomas et al.[15] reflects a difference in the measured rate constant ratios; the same value of k_{O_2} (3.2×10^{-12} cm^3 molecule^{-1} s^{-1}) was used to scale the results. The origin of this discrepancy is unclear. As discussed in Sections 3.5 and 3.6 and by Jagiella et al.[16] and Tomas et al.,[15] the atmospheric fate of the acyl radicals studied herein is addition of O_2 to form acylperoxy radicals.

4.4. Self-Reactions of Acylperoxy Radicals. The values determined in this work for the self-reaction rate constants of $(CH_3)_3CC(O)O_2$ and $(CH_3)_2CHC(O)O_2$ radicals ($k_{23} = (1.45 \pm 0.07) \times 10^{-11}$ and $k_{25} = (1.44 \pm 0.10) \times 10^{-11}$ cm^3 molecule^{-1} s^{-1}) are in excellent agreement with those measured by Tomas and Lesclaux[9] on the same apparatus using Br (instead of Cl) atoms as an initiator ($k_{23} = 1.43 \times 10^{-11}$ and $k_{25} = 1.44 \times 10^{-11}$ cm^3 molecule^{-1} s^{-1}). As noted by Tomas and Lesclaux,[9] the self-reaction kinetics of $(CH_3)_3CC(O)O_2$ and $(CH_3)_2CHC(O)O_2$ are indistinguishable from those of $CH_3C(O)O_2$, $C_2H_5C(O)O_2$, and $C_6H_5C(O)O_2$ radicals. In marked contrast to the behavior of RO_2 radicals,[26,30] the self-reaction kinetics of $RC(O)O_2$ radicals appear to be insensitive to the nature of the alkyl substituent "R". This fact is convenient when modeling the atmospheric degradation of organic compounds, which have not been the subject of detailed chemical study.

5. Conclusions

Two independent and complementary experimental techniques were used to gather a large body of self-consistent data concerning the reactions of Cl atoms with pivalaldehyde and isobutyraldehyde. These reactions proceed rapidly with rate constants that are within a factor of 4−5 of the gas kinetic limit. Abstraction of the aldehydic H atom is the major (80%−90%) reaction channel. As shown in Figure 8, when compared to the remainder of the molecule, the aldehydic H atom presents a

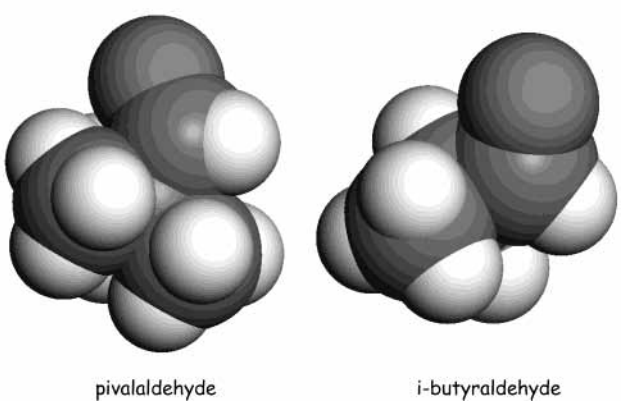

Figure 8. Molecular structures (qualitative, empirical-potential-based space-filling representations) of pivalaldehyde and isobutyraldehyde.

relatively small target for incoming Cl atoms. Given the unfavorable steric factors, the selectivity and rapidity of aldehydic H-atom abstraction is remarkable and suggests that the reaction of Cl atoms with these aldehydes probably does not proceed via a simple abstraction mechanism. Considering the electron density associated with the carbonyl group, the electrophilic nature of Cl atoms, and the proximity of the carbonyl group to the main reaction site (the aldehydic H atom), it seems reasonable to speculate that the reaction may involve a short-lived complex in which the Cl atom is associated briefly with the carbonyl group before departing with the aldehydic H atom. The resulting acyl radicals undergo both reaction with O_2 and decomposition via elimination of CO. The atmospheric fate (>98%) of acyl radicals that have been derived from pivalaldehyde and isobutyraldehyde is addition of O_2 to give the corresponding acylperoxy radical.

Acknowledgment. The authors wish to thank R. Lesclaux (University of Bordeaux) for helpful discussions, W. F. Schneider (Ford) for providing Figure 8, and the French National Program for Atmospheric Chemistry for financial support. The Nagoya group is grateful to Grants-in-Aid from the Ministry of Education, Science and Culture. The financial support by the Steel Industrial Foundation for the Advancement of Environmental Protection Technology is also gratefully acknowledged.

References and Notes

(1) Satsumabayashi, H.; Kurita, H.; Chang, Y. S.; Carmichael, G. R.; Ueda, H. *Atmos. Environ.* **1995**, *29*, 255.

(2) Viskari, E. L.; Vartiainen, M.; Pasanen, P. *Atmos. Environ.* **2000**, *34*, 917.

(3) Beine, H. J.; Jaffe, D. A.; Hering, J. A.; Kelley, J. A.; Krognes, T.; Stordal, F. *J. Atmos. Chem.* **1997**, *27*, 127.

(4) Martinez, R. D.; Buitrago, A. A.; Howell, N. W.; Hearn, C. H.; Joens, A. *Atmos. Environ., Part A* **1992**, *26*, 785.

(5) Zhu, L.; Cronin, T.; Narang, A. *J. Phys. Chem. A* **1999**, *103*, 7248.

(6) Mallard, W. G.; Westley, F.; Herron, J. T.; Hampson, R. F.; Frizzel, D. H. *NIST Chemical Kinetics Database, Version 6.0*; NIST: Gaithersburg, MD, 1997.

(7) Bartels, M.; Hoyermann, K.; Lange, U. *Ber. Bunsen−Ges. Phys. Chem.* **1989**, *93*, 423.

(8) Niki, H.; Maker, P. D.; Savage, C. M.; Breitenbach, L. P. *J. Phys. Chem.* **1985**, *89*, 588.

(9) Tomas, A.; Lesclaux, R. *Chem. Phys. Lett.* **2000**, *319*, 521.

(10) Lightfoot, P. D.; Lesclaux, R.; Veyret, B. *J. Phys. Chem.* **1990**, *94*, 700.

(11) Wallington, T. J.; Japar, S. M. *J. Atmos. Chem.* **1989**, *9*, 399.

(12) DeMore, W. B.; Sander, S. P.; Golden, D. M.; Hampson, R. F.; Kurylo, M. J.; Howard, C. J.; Ravishankara, A. R.; Kolb, C. E.; Molina, M. J. *JPL Publ.* **1997**, *97-4*.

(13) Wallington, T. J.; Andino, J. M.; Lorkovic, I. M.; Kaiser, E. W.; Marston, G. *J. Phys. Chem.* **1990**, *94*, 3644.

(14) Wallington, T. J.; Guschin, A.; Hurley, M. D. *Int. J. Chem. Kinet.* **1998**, *30*, 310.

(15) Tomas, A.; Villenave, E.; Lesclaux, R. *Phys. Chem. Chem. Phys.* **2000**, *2*, 1165.

(16) Jagiella, S.; Libuda, H. G.; Zabel, F. *Phys. Chem. Chem. Phys.* **2000**, *2*, 1175.

(17) Meagher, R. J.; McIntosh, M. E.; Hurley, M. D.; Wallington, T. J. *Int. J. Chem. Kinet.* **1997**, *29*, 619.

(18) Wine, P. H.; Semmes, D. H. *J. Phys. Chem.* **1983**, *87*, 3572.

(19) Wallington, T. J.; Hurley, M. D.; Ball, J. C.; Jenkin, M. E. *Chem. Phys. Lett.* **1993**, *211*, 41.

(20) Tyndall, G. S.; Orlando, J. J.; Wallington, T. J.; Hurley, M. D. *Int. J. Chem. Kinet.* **1997**, *29*, 655.

(21) Caralp, F.; Foucher, V.; Lesclaux, R.; Wallington, T. J.; Hurley, M. D. *Phys. Chem. Chem. Phys.* **1999**, *1*, 3509.

(22) Wallington, T. J.; Hurley, M. D.; Ball, J. C.; Kaiser, E. W. *Environ. Sci. Technol.* **1992**, *26*, 1318.

(23) Villenave, E.; Lesclaux, R. *J. Phys. Chem.* **1996**, *100*, 14372.

(24) Villenave, E.; Lesclaux, R. *J. Geophys. Res.* **1998**, *103*, 25273.

(25) Tyndall, G. S.; Cox, R. A.; Granier, C.; Lesclaux, R.; Moortgat, G. K.; Pilling, M. J.; Ravishankara, A. R.; Wallington, T. J. *J. Geophys. Res.* **2001**, *106*, 12157.

(26) Lightfoot, P. D.; Cox, R. A.; Crowley, J. N.; Destriau, M.; Hayman, G. D.; Jenkin, M. E.; Moortgat, G. K.; Zabel, F. *Atmos. Environ., Part A* **1992**, *26*, 1805.

(27) Nielsen, O. J.; Johnson, M. S.; Wallington, T. J.; Christensen, L. K.; Platz, J. *Int. J. Chem. Kinet.* **2002**, *34*, 283.

(28) Thévenet, R.; Mellouki, A.; Le Bras, G. *Int. J. Chem. Kinet.* **2000**, *32*, 676.

(29) Ullerstam, M.; Ljungstroem, E.; Langer, S. *Phys. Chem. Chem. Phys.* **2001**, *3*, 986.

(30) Wallington, T. J.; Dagaut, P.; Kurylo, M. J. *Chem. Rev.* **1992**, *92*, 667.

(31) Atkinson, R. *Int. J. Chem. Kinet.* **1997**, *29*, 99.

(32) Atkinson, R.; Baulch, D. L.; Cox, R. A.; Hampson, R. F., Jr.; Kerr, J. A.; Rossi, M. J.; Troe, J. Evaluated Kinetic and Photochemical Data for Atmospheric Chemistry, Organic Species: Supplement VII. IUPAC Subcommittee on Gas Kinetic Data Evaluation for Atmospheric Chemistry. *J. Phys. Chem. Ref. Data* **1999**, *28*, 191.

(33) Tomas, A.; Villenave, E.; Lesclaux, R. *J. Phys. Chem. A* **2001**, *105*, 3505.

(34) Wallington, T. J.; Andino, J. M.; Potts, A. R. *Int. J. Chem. Kinet.* **1992**, *24*, 649.

(35) Rowley, D. M.; Lesclaux, R.; Lightfoot, P. D.; Hughes, K.; Hurley, M. D.; Rudy, S. J.; Wallington, T. J. *J. Phys. Chem.* **1992**, *96*, 7043.